Evaluation of 1, 4, 7-Triazacyclononane (TACN) as a potential Metallo-β-Lactamase inhibitor in Enterobacteriaceae: Restoring the Activity of β-lactams

Anou M. Somboro[1, 2*], Daniel G. Amoako[1, 2], John Osei Sekyere[3], Hezekiel M. Kumalo[4], René Khan[4], Linda A. Bester[2], Sabiha Y. Essack[1]

[1]Antimicrobial Research Unit, School of Health Sciences, University of KwaZulu-Natal, Durban, South Africa;

[2]Biomedical Resource Unit, College of Health Sciences, University of KwaZulu-Natal; Durban, South Africa;

[3] Department of Medical Microbiology, Faculty of Health Sciences, University of Pretoria, South Africa;

[4]Discipline of Medical Biochemistry, School of Laboratory Medicine and Medical Science, University of KwaZulu-Natal, Durban, South Africa.

***Corresponding author:** Anou Dit Moise Somboro, Antimicrobial Research Unit, Discipline of Pharmaceutical Sciences, School of Health Sciences, University of KwaZulu-Natal, Private Bag X54001, Durban, South Africa.

Email: anou.somboro@gmail.com, Tel: +27(0) 312607671.

Running title: Inhibition of MBL by TACN

Abstract:

Metallo-β-lactamase (MBL)-producing Enterobacteriaceae are of grave clinical concern particularly as there are no MBL inhibitors approved for clinical use. The discovery and development of MBL inhibitors to restore the efficacy of available β-lactams is thus imperative. We investigated a zinc-chelating moiety, 1, 4, 7-triazacyclononane (TACN) for its inhibitory activity against clinical carbapenem-resistant Enterobacteriaceae (CRE). Minimum inhibitory concentrations, minimum bactericidal concentrations, serum effect, fractional inhibitory concentrations index and time-kill kinetics were performed using broth

micro-dilution techniques according to the CLSI guidelines. Enzyme kinetic parameters and cytotoxicity effects of TACN were determined using spectrophotometric assays. The interactions of the enzyme-TACN complex were investigated by computational studies. Meropenem (MEM) regained its activity against carbapenemase-producing Enterobacteriaceae, with the MIC decreasing to 0.03 mg/L in the presence of TACN. TACN-MEM combinations showed bactericidal effect with MIC/MBC ratio of ≤4 and synergistic activity was observed. Human serum effects on the MICs were insignificant and TACN was found to be non-cytotoxic at concentrations above the MIC values. Computational studies predicted that TACN inhibit MBLs by targeting their catalytic active site pockets. This was supported by its inhibition constant K_i = 0.044 μM and inactivation constant k_{inact} = 0.0406 (min^{-1}) demonstrating that TACN inhibits MBLs efficiently and holds promise as a potential inhibitor.

Importance of study

Carbapenem-resistant Enterobacteriaceae (CRE)-mediated infections remain a huge public health concern and have been reported as critical in the World Health Organization's Priority Pathogens List for the Research and Development of New Antibiotics. CRE produce enzymes such as Metallo-β-lactamases (MBLs), which inactivate β-lactam antibiotics. Combination therapies involving a β-lactam antibiotic and a β-lactamase inhibitor remain a major treatment option for infections caused by β-lactamase-producing organisms. Currently, no MBL inhibitor-β-lactam combination therapy is clinically available for MBL-positive bacterial infections. Hence, developing efficient molecules capable of inhibiting these enzymes remain a way forward to overcome this phenomenon. TACN played a significant role in the inhibitory activity of the tested molecules against CREs by potentiating the carbapenem. This study demonstrated that TACN inhibits MBLs efficiently and holds promise as a potential MBLs inhibitor to help curb the global health threat posed by MBL-producing CREs.

Keywords: TACN, metallo-β-lactamase inhibitor, binding affinity, β-lactams, Enterobacteriaceae

Introduction

48 β-lactams are broad-spectrum antibiotics with relatively minimal toxicity, making them antibiotics of
49 choice for many bacterial infections(1). However, the surge in resistance to β-lactams in Gram-negative
50 bacteria is affecting the management of infections worldwide(2). β-lactams are rendered ineffective
51 through different mechanisms, including reduced membrane permeability through porin down-regulation
52 and efflux, target site modification, and most importantly, the production of β-lactamases, enzymes that
53 hydrolyze β-lactams(3).

54 Metallo-β-lactamases (MBLs) are Ambler class B β-lactamases with zinc ions at their active sites. The
55 zinc ions orient a hydroxide nucleophile to attack the carbonyl on a β-lactam ring(4, 5). Sub-class B1
56 MBLs are the most clinically relevant among the class B MBLs, they possess a binuclear active site,
57 which can contain either one or two Zn (II) ions and they hydrolyze all β-lactam antibiotics in clinical
58 use with the exception of monobactams(6). MBLs such as New Delhi metallo-beta-lactamase (NDM),
59 Verona Integron-Borne Metallo-β-Lactamase (VIM) and Imipenemase (IMP) mediate high-level
60 resistance to antibiotics in carbapenem-resistant Enterobacteriaceae (CRE)(7). CRE have been
61 identified across the globe, including in all African regions(8–10) and have been ranked as critical in the
62 World Health Organization's Priority Pathogens List for the Research and Development of New
63 Antibiotics(11). It is therefore imperative to invest in the discovery and development of MBL inhibitors
64 (MBLIs) for combination therapy with carbapenems.

65 Potential MBLIs investigated to date have shown substantial *in vitro* activity but cannot be used
66 clinically due to the simultaneous inhibition of human metallo-enzymes or their cytotoxicity effects(12,
67 13). MBLIs such as aspergillomarasmine A (AMA)(13), Ca-ethylenediaminetetraacetic acid (Ca-
68 EDTA)(12), 1,4,7-triazacyclononane-1,4,7-triacetic acid (NOTA) and 1,4,7,10-tetraazacyclododecane-
69 1,4,7,10-tetraacetic acid (DOTA)(14) are the few non-toxic MBLIs identified to date and act by
70 chelating the zinc ions(15).

71 We investigated the inhibitory activity of 1, 4, 7-triazacyclononane (TACN) against well-characterized
72 sub-class B1 MBL-producing Enterobacteriaceae. TACN is a cyclic organic compound within the NOTA
73 and DOTA series and is derived from cyclononane by replacing three equidistant CH_2 groups with NH
74 groups(16) (Figure 1). We previously demonstrated NOTA and DOTA as potent MBLIs, and they
75 showed great inhibitory activity against MBL-producing Enterobacteriaceae with neither toxic nor
76 hemolytic effects at effective concentrations *in vitro*(14). To the best of our knowledge, this is the first
77 time TACN has been investigated for its inhibitory activity against MBL-producing Enterobacteriaceae to
78 potentiate the activity of meropenem (MEM).

79 **Materials and methods:**

80 **Materials**

81 MEM, TACN, dimethyl sulfoxide (DMSO), human serum, cation-adjusted Mueller-Hinton broth
82 (CAMHB) and Mueller-Hinton agar (MHA), phosphate buffered saline (PBS), β-lactamase inhibitor
83 screening kit (MAK222) and 3-(4,5-dimethylthiazol-2-yl)-2,5-diphenyltetrazolium bromide (MTT) were
84 purchased from Sigma Aldrich (St. Louis, MO, USA). Purified NDM-1 was obtained from RayBiotech,
85 Norcross, GA 30092, USA. Immortalized liver carcinoma (HepG2) cells and cell culture consumables
86 were procured from Highveld Biologicals (Johannesburg, South Africa) and Whitehead Scientific
87 (Johannesburg, South Africa) respectively.

88 **Bacterial isolates**

89 Thirty-three (33) clinical CRE strains were used for this study; these were obtained from Lancet
90 laboratories (private sector, South Africa) (Table 2)(17). Seventeen (17) carbapenem-resistant
91 Enterobacteriaceae reference isolates (including 15 MBLs and 2 SBLs) obtained from France (Institut
92 Pasteur de France) were also included in this study (Table 1)(18). *Klebsiella pneumoniae* ATCC BAA
93 1706 and *Escherichia coli* ATCC 25922 purchased from the American Type Culture Collection (ATCC)
94 were susceptible reference strains used as quality control. All bacterial isolates were fully characterized

95 in previous studies for their phenotypic and genotypic resistance profiles(17, 18). The isolates were
96 sub-cultured twice from freezer stocks onto MHA plates and incubated at 37 °C prior to the
97 experiments. All subsequent liquid subcultures were derived from colonies isolated from the agar plates
98 and were grown in broth medium (CAMHB).

99 **Methods**

100 ***Minimum Inhibitory Concentrations (MICs), Minimum Bactericidal Concentrations (MBCs)***

101 MICs/MBCs determinations were performed according to CLSI guidelines and protocols described by
102 Keepers *et al*(19, 20). Briefly, two-fold dilutions of MEM and TACN, from 0.015 to 16 mg/L and 1 to 64
103 mg/L respectively, were made with CAMHB in 96-well microtiter plates using the checkerboard
104 method(13). A 0.5 McFarland-standardized bacterial inoculum was suspended into 200 μl CAMHB in
105 each microtiter well. The plates were then incubated for 18-22 h at 37°C under aerobic conditions. The
106 MIC was determined as the lowest concentration at which there was no visible growth. Afterward, an
107 aliquot of 100 µL was taken from the MIC assay wells in which no visible growth was observed and
108 inoculated onto MHA plates for MBC determination by incubating at 37 °C for 24 h. The MBC was
109 determined as the lowest concentration of the test compound that resulted in a 99.9% decrease in
110 bacterial viable count on the agar plates. Control wells were filled with the amount of solvent(s) used in
111 dissolving drug candidates, CAMHB and bacteria. Experiments were conducted in triplicate.

112 ***Serum effects on the MIC***

113 The effects of serum on the MIC of TACN-MEM combination were performed using the above-
114 described MIC method. In this assay however, sterile-filtered serum from human male AB plasma, was
115 added to the broth (CAMHB) to prepare 50% human serum in the final culture broth. Reference CRE
116 strains carrying different enzymes (NDM-1, NDM-4, VIM-1, IMP-1 and IMP-8) were used to conduct this
117 experiment.

118 ***Synergistic activity***

119 The synergistic effect between TACN and MEM was determined by the combination assay as
120 described previously with few modifications(21). Briefly, two-fold serial dilutions of MEM were titrated
121 with a fixed concentration (8 mg/L) of TACN. This 8 mg/L TACN was the lowest concentration that did
122 not inhibit the growth of bacteria alone but considerably potentiated the activity of MEM. MEM and
123 TACN were also tested individually to determine their MICs. The fractional inhibitory concentration (FIC)
124 index was calculated as follows: FIC of MEM (MIC of MEM + TACN/MIC of MEM alone) + FIC of TACN
125 (MIC of MEM + TACN/MIC of TACN alone). The effect/activity of a combination with a FIC index of ≤
126 0.5 was considered synergistic while a FIC index of 1 was defined as additive and a FIC index of > 4
127 was characterized as antagonistic.

128 ***Time-kill assays***

129 Time-kill kinetic studies were conducted referring to the previously reported methods, including those
130 described by CLSI (19, 20). *E. coli* producing bla_{NDM-1}, *E. coli* carrying bla_{VIM-1} as well as *E. cloacae*
131 producing bla_{IMP-1} were selected for this assay. Briefly, freshly prepared colonies were re-suspended in
132 10 mL CAMHB and incubated in an orbital shaking incubator (37°C, 180 rpm) for 1 to 2 h. Cultures
133 were then adjusted to a 0.5 McFarland standard (approximately 1.5x 10^8 CFU/mL) and further diluted
134 1:20 in CAMHB so that the starting inoculum was approximately 1.5x 10^6 CFU/mL. MEM was added to
135 the prepared bacterial suspensions at final concentrations corresponding to 1x, 4x or 8x the MIC of
136 MEM whilst in combination with TACN at a fixed concentration of 8 mg/L. A growth control with no
137 antibiotic was includedin the assay. The initial bacterial load was determined from the growth control
138 test tube instantly after dilution step and was recorded as the CFU count at time zero. The test tubes
139 were incubated in an orbital shaking incubator at 37°C and 180 rpm, and bacterial cell viability counts
140 were performed at 1, 2, 4, 6, 8 and 24 hours by removing 100 µL of the culture, diluting as appropriate,
141 and plating on MHA. The agar plates were incubated at 37°C for at least 22 h. Colonies were counted,

142 and the results were recorded as the number of CFU/mL. A ≥3-log_{10} decrease in the number of
143 CFU/mL was considered bactericidal. The assays were executed in triplicate.

144 ***Cytotoxicity Assay***

145 HepG2 cells were maintained at 37°C in 10% complete culture medium (CCM; Eagles minimum
146 essential medium supplemented with fetal bovine serum, antibiotics and L-glutamine) until confluent.
147 Following trypsinization, 1.5x 10^4 cells/well were allowed to adhere to a 96-well plate overnight. The
148 cells were treated with seven dilutions of TACN (16 – 1024 mg/L) prepared in CCM. Untreated cells
149 (CCM only) served as the control. After 24 hours the treatment was replaced with 20µl MTT solution
150 (5mg/mL MTT in PBS) and 100µl CCM for 4 hours. The resulting formazan product was solubilized in
151 100µl DMSO (1 hour) and the absorbance at 570nm/690nm was determined (BioTek µQuant plate
152 reader; BioTek Instruments Inc., USA). The average absorbance values were used to calculate cell
153 viability ($\frac{Absorbance\ of\ treatment}{Absorbance\ of\ control}\ x\ 100$) and determine the IC_{50} (GraphPad Prism® v5.01). All
154 experiments were performed in triplicate.

155 ***Enzymatic assays: Enzyme inhibition and inactivation kinetic parameters***

156 The inhibitory effect of TACN was monitored by observing the rate of hydrolysis of the chromogenic
157 nitrocefin, using purified preparations of sub-class B1 MBL enzyme (NDM-1) obtained from Raybiotech
158 (Norcross, GA 30092, USA). The assays were performed using the β-lactamase inhibitor screening kit's
159 (MAK222) according to the manufacturer's instructions. Briefly, 5 nM of NDM-1 was pre-incubated with
160 various concentrations of TACN varying from 0 - 50 µM at 25°C in a final experimental volume of 100
161 µL of β-lactamase assay buffer prior to adding nitrocefin. The nitrocefin hydrolysis was monitored at
162 25°C by following the absorbance variation at 490nm using a plate reader spectrophotometer
163 (SPECTROstar^{Nano} BMG Labtech, Germany). The residual activity was determined and compared to
164 that from the pre-incubation of the enzyme with the same procedure, but without TACN. The effect of

165 TACN-mediated inactivation of NDM-1 was determined by plotting the natural logarithm (LN)-linear plot
166 of the percentage of the remaining enzyme residual activity versus the pre-incubation time, and the
167 observed initial inactivation rate constant (K_{obs}) was calculated from the pseudo-first-order kinetic slope.
168 The rate constant for enzyme inactivation (k_{inact}) and the inactivation constant (K_I) were calculated
169 (GraphPad Prism5; Software Inc., San Diego, CA) according to the following hyperbolic equation as
170 previously described by Wong *et al.* (22):

$$Kobs = \frac{Kinact - [I]}{Ki + [I]}$$

171 Where K_{obs} is the initial rate constant for TACN inactivation and [I] is the initial inhibitor concentration.

172 The preliminary mode of inhibition of NDM-1 by TACN was also assessed using the β-lactamase
173 inhibitor screening kit reagents. Briefly, 500 nM of purified NDM-1 was pre-incubated with 20 μM of
174 TACN at 25°C for 20 min, followed by rapid dilution with the addition of 30 μM of nitrocefin; after which,
175 changes in absorbance were monitored at 490 nm for 30 min. Experiments were conducted in triplicate.

176 ***Molecular modelling***

177 ***System preparation***

178 The crystal structures (PDB ID: 3Q6X, and 5ACU) were retrieved from the RSCB Protein Data Bank
179 (https://www.rcsb.org/pdb/). The missing residues were added using a graphical user interface of
180 Chimera, a molecular modelling tool(23). A ligand interaction map was generated using the web version
181 of PoseView(24).

182 ***Molecular Docking***

183 Docking calculations were obtained using AutoDock Vina software(25). Geister partial charges were
184 assigned and the AutoDock atom types were defined using the AutoDock graphical user interface
185 supplied by MGL tools(26). The docked conformations were generated using the Lamarckian genetic

186 algorithm (LGA)(27). The reports for each calculation were in Kcal/mol. This technique has been
187 validated in previous studies(28). The grid box was defined using Autodock Vina with the grid
188 parameters being X= 26, Y= 18 and Z= 20 for the dimensions and X= -2.502, Y= -5.255 and Z= 32.723
189 for the center grid box. After using Autodock Vina, the 10 conformations with lowest binding energy was
190 chosen for molecular docking.

191 ***Molecular dynamics simulation***

192 Missing parameters for the ligand in the Cornell et al. force field were created (29) in the absence of
193 available parameters. Optimization of the ligands was first performed at the HF/6-31G* level with the
194 Gaussian 03 package. The restrained electrostatic potential (RESP) procedure(30) was used to
195 calculate the partial atomic charges. General amber force GAFF(31) force field parameters and RESP
196 partial charges were assigned using the ANTECHAMBER module in the Amber14 package. Hydrogen
197 atoms of the proteins were added using the Leap module in Amber12. The standard AMBER force field
198 for bioorganic systems (ff03) was used to define the enzyme parameters. Counter ions were added to
199 neutralize the enzyme charge. The system was enveloped in a box of equilibrated TIP3P water
200 molecules with 8 Å distance around the enzyme. Cubic periodic boundary conditions were imposed and
201 the long-range electrostatic interactions were treated with the particle-mesh Ewald method (32)
202 implemented in Amber12 with a non-bonding cut-off distance of 10 Å.

203 Initial energy minimization, with a restraint potential of 2 kcal/mol $Å^2$ applied to the solute, was carried
204 out using the steepest descent method in Amber12 for 1000 iterations followed by conjugate gradient
205 protocol for 2000 steps. The entire system was then freely minimized for 1000 iterations. Harmonic
206 restraints with force constants 5 kcal/mol $Å^2$ were applied to all solute atoms during the heating phase.
207 A canonical ensemble constant number (N), volume (V), and temperature (NVT) MD was carried out for
208 50 ps, during which the system was gradually annealed from 0 to 300 K using a Langevin thermostat
209 with a coupling coefficient of 1/ps. Subsequently, the system was equilibrated at 300 K with a 2 fs time

210 step for 100 ps whilst maintaining the force constants on the restrained solute. The SHAKE
211 algorithm(33) was employed on all atoms covalently bonded to a hydrogen atom during equilibration
212 and production runs. A production run was performed for 2 ns in an isothermal isobaric (NPT) ensemble
213 using a Berendsen barostat(34) with a target pressure of 1 bar and a pressure coupling constant of 2
214 ps with no restraints imposed. The coordinate file was saved every 1 ps and the trajectory was
215 analyzed every 1 ps using Ptraj module implemented in Amber14.

216 **Results**

217 ***MICs, MBCs, MIC/MBC ratio***

218 TACN successfully restored the activity of MEM against characterized clinical isolates of CRE
219 expressing acquired sub-class B1 carbapenemases and MBL reference strains at concentrations as
220 low as 0.03 mg/L. Different concentrations of TACN considerably enhanced the efficacy of MEM
221 against the MBL-producing bacteria (varying from 2-64 mg/L). The lowest concentration of TACN at
222 which most of the MEM activity was restored was 8 mg/L. All subsequent experiments were therefore
223 conducted with a fixed concentration of 8 mg/L. None of the tested serine β-lactamases (SBLs) types
224 (*K. pneumonia* OXA-48 and *E. cloacae* KPC-2) were affected by TACN, substantiating the substrate
225 spectrum of this compound. MBCs of MEM were determined in the presence of TACN at a fixed
226 concentration and the MBC/MIC ratio of the combination ranged from 1- to 4-fold against both
227 reference and clinical CRE isolates used in this study, with the exception of two clinical isolates, which
228 had 8x the MIC values (Table 2). *K. pneumoniae* ATCC BAA 1706 and *E. coli* ATCC 25922 had no
229 changes in their MIC values when challenged with MEM alone and MEM+TACN.

230 ***Serum effect on MIC***

231 The MIC values of MEM-TACN combinations in the presence of 50% human serum varied from ±1- to
232 4-fold dilutions compared to that of MEM-TACN in the absence of serum indicating that the inhibition
233 properties of the combination were not affected by the presence of human serum (Table 1).

234 ***Synergistic effect of TACN and MEM on CRE reference strains***

235 Synergy between TACN and MEM against CRE isolates was investigated. In most of the cases, the
236 minimum concentrations of TACN alone required to inhibit the MBL-producing Enterobacteriaceae were
237 ≥128mg/L (Table 1). MEM alone exhibited inhibitory concentrations of ≥8mg/L, indicating carbapenem-
238 resistant phenotype of these pathogens(20). Challenging these CREs with a combined regimen of
239 MEM-TACN potentiated the effectiveness of MEM. The calculated FIC index of MEM-TACN was ≤0.5,
240 indicating a synergistic effect (Table 1).

241 ***Time-kill kinetics***

242 The combination of MEM-TACN caused a considerable decrease in the CFU/mL relative to the initial
243 bacterial density of approximately 10^6 CFU/mL) over the increasing time points (0, 1, 2, 4, 6, 8 and 24
244 h) against the tested isolates at different concentrations of the MIC values evaluated in this study (1x,
245 4x, 8x MICs) (Figure 2). A $3\log_{10}$ decrease in the CFU/ml was observed when cells were treated with
246 MEM-TACN at 1x, 4x and 8x MICs at 4 h. The time-kill kinetics results indicated that the TACN-MEM
247 combinations had bactericidal activity against the selected CRE isolates.

248 ***Cytotoxicity***

249 The MTT assay was used to measure TACN cytotoxicity (0 – 1024mg/L) in HepG2 cells after 24-hour
250 exposure. A decrease in cell viability was associated with an increase in TACN concentration (Figure 3)
251 and the regression analysis yielded an IC_{50} of 56 mg/L. However, this IC_{50} of TACN was far higher than
252 the fixed MIC value of 8 mg/L used in this study.

253 ***Enzymatic assays***

254 TACN efficiently inhibited the activity of NDM-1 in a concentration- and time-dependent manner
255 illustrated by Figure 4A where the effect of increasing concentrations of TACN (0 – 50 μM) on the time-
256 dependent decrease in NDM-1 activity. The kinetic parameters were constructed by nonlinear

257 regression of the K_{obs} versus TACN concentration plot shown in figure 4B. TACN was found to be a
258 potent time-dependent inhibitor with inhibition constant K_i and the inactivation constant K_{inact} of
259 0.044±018 μM and 0.0406 ±0.007 (min^{-1}) respectively.

260 ***Computational simulations***

261 The fluctuations of enzyme-ligand complex and ligand-associated movements were analyzed to
262 ascertain their structural stability and movements during the course of simulation. These movements,
263 which ensure their functional reliability and working efficiency, are important for functionality and
264 existence inside the living system. The overall systems showed appreciable stability as depicted in
265 Figure 6. The root-mean-square deviation (RMSD) of the entire systems complex remained stable
266 during the course of simulation of 100 ns.

267 The calculated binding free energy of TACN to NDM-1 and VIM-2 by the Molecular
268 Mechanics/Poisson−Boltzmann Surface Area *(MM/GBSA) protocol is shown in Table 3. The calculated
269 contributions favoring the inhibitors' binding include the electrostatic interactions (Δ Eele), which were -
270 9.4229 kcal/mol for NDM-1_{TACN} complex. The intermolecular van der Waals energy (Δ Evdw) for NDM-
271 1_{TACN} was -46.0898 kcal/mol, also favoring binding. The total binding free energies (Δ Gbind) for NDM-
272 1_{TACN} was -39.1603 kcal/mol. A similar trend was also observed with the complex VIM-2_{TACN} as shown
273 in table 3. The results suggest that the theoretical calculations of the binding free energies support the
274 experimental findings in term of potentiality of TACN to inhibit the MBL enzymes.

275 To gain further understanding of the active-site residue interactions with the compounds, the simulated
276 complexes were observed with LigPlot protein-ligand interaction software. It was observed that the
277 ligand is attached with the active site residues in all complexes as shown in Figure 7. For TACN,
278 His250, Asp124 residues provided H-bonding capability whilst His122, Asn220 and Trp93 roof the
279 hydrophobic active-site pocket. These residues are providing the hydrophobic surface area whilst
280 maintaining H-bonding capability.

281 **Discussion**

282 This study evaluated the TACN-MEM combination against clinical and reference CRE isolates and
283 identified TACN as a promising MBLI. The affinity of metal chelators for binding/sequestering metal
284 ions(35) such as zinc at MBLs' active sites makes them potential inhibitors that can be developed for
285 treating CRE infections. TACN is a metal chelating agent that exhibited no cytotoxic effect at effective
286 concentrations.

287 We showed that TACN significantly reduced the MIC of MEM, reinstating the carbapenem's efficacy
288 against thirty-three (33) South African clinical isolates and 15 MBL-producing reference strains. MEM
289 MICs decreased by 4- to >512-fold changes in the presence of TACN against all the tested isolates,
290 except for SBL producers and susceptible ATCC strains. The SBL-producing *E. cloacae* KPC-2 and *K.*
291 *pneumoniae* OXA-48 only exhibited 2 or no fold decrease in MEM MICs, showing that the inhibitory
292 effect of TACN was specific for zinc-based β-lactamases. In our previous study NOTA and DPA
293 exhibited similar activity against MBLs at 4 and 8 mg/L(14, 36). Metal chelators are known for their
294 strong affinity toward metal ions(35). Class B MBLs possess zinc at their active sites, thus enabling the
295 TACN to bind or sequester the zinc ions and inhibit the enzymes' β-lactam hydrolysis activity.

296 MEM regained its pharmacological properties when combined with TACN. Most of the tested isolates
297 exhibited MBC/MIC ratio of ≤ 4, except for 2 clinical isolates, *S. marcescens and E. cloacae,* where the
298 MBC/MIC ratio was 8 (Table 2). Based on the MBC/MIC ratio values, MEM demonstrated its known
299 bactericidal activity in the presence of TACN and time-kill kinetic studies confirmed the bactericidal
300 property of MEM-TACN combinations. The MEM-TACN combination was synergistic, with an FIC index
301 ranging from ≤ 0.005 to 0.25 for all the CRE reference strains used in the study. Aspergillomarasmine
302 A, a metal chelating agent, was also found synergistic in combination with MEM toward MBLs(37).

303 The results also showed that serum had no substantial effect on the MICs of TACN-MEM combinations.
304 The minimal or no effects of serum on the activity of MEM was attributed to MEM's low protein-binding

305 properties(38). An investigation of the effects of serum on TACN or MEM's MICs may allow speculation
306 on the probable *in vivo* properties of the molecules at pre-clinical stage. Furthermore, TACN did not
307 affect the pharmacological property of MEM, suggesting that TACN could have low plasma protein-
308 binding properties either with or without MEM.

309 The MTT assay measures the ability of cells to reduce the MTT salt to a formazan product (39). This
310 reaction can only occur in living cells with healthy mitochondria, as it is reliant on NADPH-dependent
311 oxidoreductase enzymes. The cell viability obtained therefore reflects the number of viable cells
312 present. TACN exposure resulted in a dose-dependent decrease in cellular metabolic activity and
313 viability in HepG2 cells (Figure 3). However, the IC_{50} obtained was ≥4-fold higher than the TACN
314 inhibitory dose (8mg/L) and the cell viability was 91% at the upper limit of the inhibitory dose. This
315 cytotoxicity analysis on TACN found the compound possessing tolerable toxicity on HepG2 cell line at
316 the applied concentration, hence showing potential for development as MBLI for clinical use.

317 An experimental assay together with computational simulation demonstrated good binding affinity
318 between ligand and enzyme complexes as well as potential inhibitory properties. It is known that Class
319 B β-lactamases are susceptible to inhibition by chelating agents during interactions between the
320 chelators (ligands) and the metal ions after ions are released from the proteins (MBL) active site or
321 while still associated with the enzyme complex(40). TACN possessed an apparent potential inhibition
322 property toward NDM-1 enzyme like Aspergillomarasmine A(37) as shown in figure 5. Overall, the
323 calculated variation of RMSD did not show considerable structural shifts, suggesting the stability of the
324 enzyme structure and strength of ligand attachment inside the active site pocket. The binding free
325 energy analysis showed that the intermolecular van der Waals and the electrostatic interaction were the
326 forces driving both systems. However, the total solvation energy (ΔGsol) was unfavorable for all the
327 complexes. Even though hydrogen bonds between the ligand and receptors were observed using
328 LigPlot and chimera (Figure 7), their influences could not compensate for the large desolvation
329 penalties during the interaction, thereby leading to the total solvation energy (ΔGsol). Similar results

330 have been reported previously where inhibition was dominated by the van der Waals interactions (41,
331 42).

332 This study showed that TACN inhibits Class B1 MBL-producing CREs with minimal cytotoxic effect at
333 effective concentrations. TACN successfully potentiated the antimicrobial properties of MEM as should
334 thus be further investigated as a MBLI for clinical development, in combination with carbapenems.
335 Molecular modeling and docking studies demonstrated the mechanistic pathway of TACN to inhibit
336 NDM-1 and VIM-2 sustaining a stable enzyme-ligand complex with the caveat that this is only
337 simulation of a prediction and not likely to represent the actual binding mode. In-depth analysis and
338 optimization of the metal-chelating agent (TACN), employing a multidisciplinary research approach
339 involving advanced computational simulations, biochemical, microbiological, bio-informatics are needed
340 in order to provide more evidence.

341 **Author contributions:**

342 Co-conceptualized the study: AMS, DGA, JOS, LAB and SYE. Performed the experiments: AMS, DGA,
343 HMK and RK. Analyzed the data: AMS, DGA, HMK and RK. Vetting of the results: All. Wrote the paper:
344 AMS. Undertook critical revision of the manuscript: All

345 **Acknowledgment:** We are grateful to the South African National Research Foundation (**Grant No.:**
346 **85595** awarded to Professor S.Y. Essack as Incentive Funding for Rated Researchers) and College of
347 Health Sciences, UKZN, for funding this study.

348 **Funding information:** The College of Health Sciences, University of Kwa-Zulu Natal, Durban, South
349 Africa and the South African National Research Foundation (NRF) supported this study.

350 **Conflict of Interest:** No conflict of interest

351 **References**

352 1. Wilke MS, Lovering AL, Strynadka NCJ. 2005. Beta-Lactam antibiotic resistance: A current

353 structural perspective. Curr Opin Microbiol 8:525–533.

354 2. Gaude G, Hattiholli J. 2013. Rising bacterial resistance to beta-lactam antibiotics: Can there be
355 solutions? J Dr NTR Univ Heal Sci 2:4–9.

356 3. Heesemann J. 1993. Mechanisms of resistance to beta-lactam antibiotics. Infection 21:S4-9.

357 4. Hall BG, Salipante SJ, Barlow M. 2003. The metallo-β-lactamases fall into two distinct
358 phylogenetic groups. J Mol Evol 57:249–254.

359 5. Garau G, García-Sáez I, Bebrone C, Anne C, Mercuri P, Galleni M, Frère JM, Dideberg O.
360 2004. Update of the standard numbering scheme for class B β-lactamases. Antimicrob Agents
361 Chemother 48:2347–2349.

362 6. Walsh TR, Toleman MA, Poirel L, Nordmann P. 2005. Metallo-β-lactamases: The quiet before
363 the storm? Clin Microbiol Rev 18:306–325.

364 7. Falconer SB, Reid-Yu SA, King AM, Gehrke SS, Wang W, Britten JF, Coombes BK, Wright GD,
365 Brown ED. 2016. Zinc Chelation by a Small-Molecule Adjuvant Potentiates Meropenem Activity
366 in Vivo against NDM-1-Producing Klebsiella pneumoniae. ACS Infect Dis 1:533–543.

367 8. Gupta N, Limbago BM, Patel JB, Kallen AJ. 2011. Carbapenem-resistant enterobacteriaceae:
368 Epidemiology and prevention. Clin Infect Dis 53:60–67.

369 9. Sekyere JO, Govinden U, Essack S. 2016. The Molecular Epidemiology and Genetic
370 Environment of Carbapenemases Detected in Africa. Microb Drug Resist 22:59–68.

371 10. Osei Sekyere J. 2016. Current State of Resistance to Antibiotics of Last-Resort in South Africa:
372 A Review from a Public Health Perspective. Front Public Heal 4:209.

373 11. World Health Organization. 2017. Global Priority List Of Antibiotic-Resistant Bacteria To Guide
374 Research, Discovery, And Development Of New Antibiotics.

375 12. Yoshizumi A, Ishii Y, Livermore DM, Woodford N, Kimura S, Saga T, Harada S, Yamaguchi K,
376 Tateda K. 2013. Efficacies of calcium-EDTA in combination with imipenem in a murine model of
377 sepsis caused by Escherichia coli with NDM-1 Beta-lactamase. J Infect Chemother 19:992–995.

378 13. King AM, Reid-Yu SA, Wang W, King DT, De Pascale G, Strynadka NC, Walsh TR, Coombes
379 BK, Wright GD. 2014. Aspergillomarasmine A overcomes metallo-β-lactamase antibiotic
380 resistance. Nature 510:503–506.

381 14. Somboro AM, Tiwari D, Bester LA, Parboosing R, Chonco L, Kruger HG, Arvidsson PI,
382 Govender T, Naicker T, Essack SY. 2014. NOTA: A potent metallo-β-lactamase inhibitor. J
383 Antimicrob Chemother 70:1594–1596.

384 15. McGeary RP, Tan DT, Schenk G. 2017. Progress toward inhibitors of metallo-β-lactamases.
385 Future Med Chem 9:673–691.

386 16. Weighardt P. & Chaudhuri K. 1987. The Chemistry of 1,4,7-Triazacyclononane and Related
387 Tridentate Macrocyclic Compounds. Prog Inorg Chem 35:329–436.

388 17. Osei Sekyere J, Amoako DG. 2017. Genomic and phenotypic characterisation of
389 fluoroquinolone resistance mechanisms in Enterobacteriaceae in Durban, South Africa. PLoS
390 One 12:e0178888.

391 18. Nordmann P, Poirel L, Dortet L. 2012. Rapid detection of carbapenemase-producing
392 enterobacteriaceae. Emerg Infect Dis 18:1503–1507.

393 19. Keepers TR, Gomez M, Celeri C, Nichols WW, Krause KM. 2014. Bactericidal activity, absence
394 of serum effect, and time-kill kinetics of ceftazidime-avibactam against Beta-lactamase-
395 producing Enterobacteriaceae and Pseudomonas aeruginosa. Antimicrob Agents Chemother
396 58:5297–5305.

397 20. Clinical and Laboratory Standards Institute. 2017. Performance Standards for Antimicrobial
398 Susceptibility Testing: 27th edition Informational Supplement M100-S27. CLSI, Wayne, PA,
399 USA.

400 21. Pankey GA, Ashcraft DS. 2005. In vitro synergy of ciprofloxacin and gatifloxacin against
401 ciprofloxacin-resistant Pseudomonas aeruginosa. Antimicrob Agents Chemother 49:2959–2964.

402 22. Wong SG, Fan PW, Subramanian R, Tonn GR, Henne KR, Johnson MG, Lohr MT, Wong BK.
403 2010. Bioactivation of a novel 2-methylindole-containing dual chemoattractant receptor-
404 homologous molecule expressed on T-helper type-2 cells/D-prostanoid receptor antagonist
405 leads to mechanism-based CYP3A inactivation: glutathione adduct characterization and
406 prediction of in vivo drug-drug interaction. Drug Metab Dispos 38:841–850.

407 23. Pettersen EF, Goddard TD, Huang CC, Couch GS, Greenblatt DM, Meng EC, Ferrin TE. 2004.
408 UCSF Chimera—A Visualization System for Exploratory Research and Analysis. J Comput
409 Chem 25:1605–1612.

410 24. Stierand K, Rarey M. 2010. PoseView - molecular interaction patterns at a glance. J
411 Cheminform 2:50.

412 25. Trott O, Olson AJ. 2010. Software news and update AutoDock Vina: Improving the speed and
413 accuracy of docking with a new scoring function, efficient optimization, and multithreading. J
414 Comput Chem 31:455–461.

415 26. Sanner MF. 1999. Python: a programming language for software integration and development. J
416 Mol Graph Model 17:57–61.

417 27. Huey R, Morris GM, Olson AJ, Goodsell DS. 2007. Software news and update a semiempirical
418 free energy force field with charge-based desolvation. J Comput Chem 28:1145–1152.

419 28. Kumalo HM, Soliman ME. 2016. Per-Residue Energy Footprints-Based Pharmacophore
420 Modeling as an Enhanced In Silico Approach in Drug Discovery: A Case Study on the
421 Identification of Novel β-Secretase1 (BACE1) Inhibitors as Anti-Alzheimer Agents. Cell Mol
422 Bioeng 9:175–189.

423 29. Cornell WD, Cieplak P, Bayly CI, Gould IR, Merz KM, Ferguson DM, Spellmeyer DC, Fox T,
424 Caldwell JW, Kollman PA. 1995. A Second Generation Force Field for the Simulation of
425 Proteins, Nucleic Acids, and Organic Molecules. J Am Chem Soc 117:5179–5197.

426 30. Cieplak P, Cornell WD, Bayly C, Kollman PA. 1995. Application of the multimolecule and
427 multiconformational RESP methodology to biopolymers: Charge derivation for DNA, RNA, and
428 proteins. J Comput Chem 16:1357–1377.

429 31. Wang J, Wolf RM, Caldwell JW, Kollman PA, Case DA. 2004. Development and testing of a
430 general Amber force field. J Comput Chem 25:1157–1174.

431 32. Essmann U, Perera L, Berkowitz ML, Darden T, Lee H, Pedersen LG. 1995. A smooth particle
432 mesh Ewald method. J Chem Phys 103:8577–8593.

433 33. Ryckaert JP, Ciccotti G, Berendsen HJC. 1977. Numerical integration of the cartesian equations
434 of motion of a system with constraints: molecular dynamics of n-alkanes. J Comput Phys
435 23:327–341.

436 34. Berendsen HJC, Postma JPM, van Gunsteren WF, DiNola A, Haak JR. 1984. Molecular
437 dynamics with coupling to an external bath. J Chem Phys 81:3684–3690.

438 35. Zhang Y, Hong H, Engle JW, Bean J, Yang Y, Leigh BR, Barnhart TE, Cai W. 2011. Positron
439 Emission Tomography Imaging of CD105 Expression with a 64Cu-Labeled Monoclonal
440 Antibody: NOTA Is Superior to DOTA. PLoS One 6:e28005.

441 36. Azumah R, Dutta J, Somboro AM, Ramtahal M, Chonco L, Parboosing R, Bester LA, Kruger
442 HG, Naicker T, Essack SY, Govender T. 2016. In vitro evaluation of metal chelators as potential
443 metallo- β -lactamase inhibitors. J Appl Microbiol 120:860–867.

444 37. King AM, Reid-Yu SA, Wang W, King DT, De Pascale G, Strynadka NC, Walsh TR, Coombes
445 BK, Wright GD. 2014. Aspergillomarasmine A overcomes metallo-β-lactamase antibiotic
446 resistance. Nature 510:503–506.

447 38. Craig WA, Welling PG. 1977. Protein Binding of Antimicrobials: Clinical Pharmacokinetic and
448 Therapeutic Implications. Clin Pharmacokinet 2:252–268.

449 39. Mosmann T. 1983. Rapid colorimetric assay for cellular growth and survival: Application to
450 proliferation and cytotoxicity assays. J Immunol Methods 65:55–63.

451 40. Viswanatha T, Marrone L, Goodfellow V, Dmitrienko GI. 2008. Assays for beta-lactamase
452 activity and inhibition. Methods Mol Med 142:239–260.

453 41. Liang Z, Li L, Wang Y, Chen L, Kong X, Hong Y, Lan L, Zheng M, Guang-Yang C, Liu H, Shen
454 X, Luo C, Li KK, Chen K, Jiang H. 2011. Molecular basis of NDM-1, a new antibiotic resistance
455 determinant. PLoS One 6:e23606.

456 42. Meini M-R, Llarrull L, Vila A. 2014. Evolution of Metallo-β-lactamases: Trends Revealed by
457 Natural Diversity and in vitro Evolution. Antibiotics 3:285–316.

458

459 **Table 1:** Inhibitory activity of TACN and MEM alone and in combination against reference strains of
460 carbapenem-resistant Enterobacteriaceae.

Bacterial species	Metallo-β-lactamase (MBLs) produced (Class B)	MIC (mg/L)			MBC (mg/L)	MIC/MBC (mg/L)	Serum (mg/L)	effect	FIC index
		MEM	TACN	{MEM-TACN}	MEM-TACN8*	MEM-	MEM-		

						TACN8	TACN8/Serum	
Zinc-metallo-β-lactamases								
E. coli	NDM-1	128	1024	{0.125-4} {0.125-8} {0.06-16}	0.5	2	0.25	0.008
E. cloacae	NDM-1	16	>1024	{0.125-2} {0.06-4} {0.03-8}	0.125	2	0.125	≤0.005
C. freundii	NDM-1	8	1024	{0.25-4} {0.125-8} {0.125-16}	0.125	1	0.25	0.023
P. rettgeri	NDM-1	64	>1024	{8-4} {2-8}	2	1	2	≤0.035
P. stuartii	NDM-1	16	>1024	{2-4} {2-8}	2	1	4	≤0.253
E. coli	NDM-4	128	1024	{0.125-8} {0.06-16}	0.125	1	1	0.008
E. coli	VIM-1	32	1024	{0.25-4} {0.125-8} {0.06-16}	0.125	1	0.25	0.011
K. pneumoniae	VIM-1	32	512	{2-4} {0.125-8} {0.06-16}	0.5	4	8	0.019
E. cloacae	VIM-1	8	128	{1-4} {1-8}	1	1	2	0.187
E. coli	VIM-2	8	128	{0.06-4} {0.03-8}	0.06	1	0.125	0.066
E. cloacae	IMP-1	32	512	{0.25-4} {0.125-8}	0.5	2	2	0.019
K. pneumoniae	IMP-1	32	512	{8-4} {4-8}	4	1	16	0.141
E. coli	IMP-1	16	512	{1-4} {0.06-8} {0.03-16}	0.125	2	0.25	0.019
E. cloacae	IMP-8	8	512	{0.5-4} {0.125-8} {0.03-16}	0.25	2	0.125	0.031
K. pneumoniae	IMP-8	16	1024	{8-4} {4-8} {2-16}	8	2	4	0.250
Serine-metallo-β-lactamases								
K. pneumoniae	OXA-48	8	128	{8-8} {8-16} {4-64}	NA**	NA	NA	NA
E. cloaeae	KPC-2	32	256	{32-32} {32-64}	NA	NA	NA	NA
Susceptible ATCC strains								
K. pneumoniae ATCC BAA 1706	Susceptible strain	0.5	1024	NE***	NA	NA	NA	NA
E. coli ATCC 25922	Susceptible strain	0.03	1024	NE	NA	NA	NA	NA

461 *Fixed concentration of TACN (8 mg/L)
462 **Not applicable
463 *** No inhibitory effect
464

465 **Table 2**: Minimal inhibitory concentrations (MIC) and minimal bactericidal concentrations (MBC) of
466 TACN against South African clinical isolates.

Bacterial species and isolates	MBLs produced (Class B)	Other β-lactamase (s)	MIC (mg/L)	MBC (mg/L)	MIC/MBC ratio (mg/L)
			MEM with TACN	MEM with TACN	MEM with TACN
K. pneumoniae (N=11)					
D(UNN40_S4)	NDM-1	DHA-1, CTX-M-15, SHV-1, OXA-1	0.5	2	4
C(UNN39_S3)	NDM-1	SHV-1, CTX-M-15, OXA-1, DHA-1	0.5	2	4

Bacterial species and isolates	MBLs produced (Class B)	Other β-lactamase (s)	MIC (mg/L)	MBC (mg/L)	MIC/MBC ratio (mg/L)
			MEM with TACN	MEM with TACN	MEM with TACN
I(UNN45_S9)	NDM-1	OXA-1, CTX-M-15, SHV-99, TEM-1B	4	8	2
J(UNN46_S10)	NDM-1	OXA-1, CTX-M-15, SHV-1&-28, DHA-7	0.5	2	4
53_S27	NDM-1	OXA-1, DHA-1, CTX-M-15, SHV-1&-28,	4	16	4
12_S5	NDM-1	CTX-M-15, SHV-1&-28, DHA-1, OXA-1	2	8	4
13_S6	NDM-1	CTX-M-15, SHV-1&-28, DHA-7	4	16	4
20_S11	NDM-1	CTX-M-15, TEM-1A, OXA-9, SHV-1&-28, OXA-1&-9	0.125	1	4
29_S13	NDM-1	CTX-M-15, SHV-1&-28, OXA-1&-9, TEM-1A	0.125	1	4
32_S15	NDM-1	DHA-1, CTX-M-15, SHV-1&-28, OXA-1	0.125	1	4
21_S12	NDM-1	TEM-1A, SHV-1&-28, CTX-M-15, OXA1&-9	0.5	1	2
S. marcescens (N=10)					
B(UNN38_S2)	NDM-1	OXA-10, OXA-1, CTX-M-15, SCO-1, TEM-133, TEM-198	0.125	1	4
E(UNN41_S5)	NDM-1	CTX-M-15, SCO-1, TEM-198, OXA-10, OXA - 1	1	2	2
G(UNN43_S7)	NDM-1	OXA-10, TEM-1B	1	4	4
K(UNN47_S11)	NDM-1	TEM-1B, OXA-1, OXA-10, SCO-1	2	16	8
L(UNN48_S12)	NDM-1	CTX-M-15, OXA-10, OXA -1, SCO-1, TEM-1	2	4	2
7_S3	NDM-1	TEM- 1B, OXA-10	2	8	4
56_S29	NDM-1	NONE	0.5	2	4
59_S30	NDM-1	TEM-1B, CTX-M-3	1	2	2
67_S33	NDM-1	OXA-10, CTX-M -15, OXA-1, TEM-1, SCO-1	4	16	4
71_S36	NDM-1	CTX-M-11, TEM -1B, OXA -10, OXA-1, SCO-1	2	2	1
E. cloacae (N=9)					
A(UNN37_S1)	NDM-1	CTX-M-3, ACT-3	0.5	1	2
F (UNN42_S6)	NDM-1	CTX-M-15, TEM -1B, OXA-1, ACT-7	0.5	2	4
H(UNN44_S8)	NDM-1	CTX-M-15, TEM -1B, OXA-1, ACT-14	1	1	1
16_S9	NDM-1	CTX-M-15, OXA-1, ACT-4,	0.125	2	8
43_S20	NDM-1	TEM -1B, SHV-12, MIR-1	2	4	2
49_S24	NDM-1	CTX-M-15, TEM-1B, OXA-1, ACT-3, CMY-77	0.5	1	2
51	NDM-1	CTX-M-3, TEM-1B, CMY-77	0.25	1	4
55_S28	NDM-1	TEM -1B, ACT-4, SHV-12	4	2	2
63_S31	NDM-1	TEM-1B, ACT-1	0.5	2	4
E.coli (N=1)					
10	NDM-5	CMY-42	2	4	2
C. freundii (N=1)					

Bacterial species and isolates	MBLs produced (Class B)	Other β-lactamase (s)	MIC (mg/L)	MBC (mg/L)	MIC/MBC ratio (mg/L)
			MEM with TACN	MEM with TACN	MEM with TACN
48	NDM-1	CTX-M-3, TEM-1B, CMY-77	0.25	2	4
K.oxytoca (N=1)					
69	NDM-1	CTX-M-3, TEM-1B, OXY-14	0.25	2	4

467

468 **Table 3**: MM/GBSA binding free energy profile for $NMD1_{TACN}$, and $VIM\text{-}2_{TCN}$

Binding free energy profile					
Systems	**Evdw**	**Eelec**	**ΔGsolv**	**ΔGgas**	**ΔGbind**
$NDM\text{-}1_{TACN}$ complex	-46.0898	-9.4229	16.3523	-55.5126	-39.1603
$VIM\text{-}2_{TACN}$ complex	-50.9300	-9.9143	19.6230	-63.4178	-41.2199

469 ΔG_{bind}- binding energy; ΔE_{ele} – electrostatic; ΔE_{vdw} – van der waals; ΔE_{gas} - gas-phase energy; ΔE_{sol} – solvation energy

470 **List of figures**

471 **Figure 1:** Chemical structure of 1, 4, 7-triazacyclononane (TACN)

472 **Figure 2:** Time kill kinetics at varying concentrations of MEM and fixed concentration of TACN (8
473 mg/mL). A) *E. coli* producing NDM-1; B). *E. coli* producing VIM-1; C) *E. cloacae* producing IMP-1 were
474 challenged at 1x, 4x and 8x MIC levels with MEM-TACN combination. The surviving CFU were plated
475 at different time intervals (1, 2, 4, 6, 8, 24 hours). All data points represent the average results for 3
476 independent experiments.

477 **Figure 3:** TACN induced a dose-dependent decrease in HepG2 cell viability following treatment for 24-
478 hour treatment. Higher TACN concentrations resulted in increased cell death.

479 **Figure 4:** A) Time- and concentration-dependent inhibition of NDM-1 by TACN, B) The logarithmic plot
480 of kobs of TACN against TACN concentrations.

481 **Figure 5:** Residual activity after rapid dilution of enzyme-inhibitor complex. The absorbance changes
482 from the co-incubation of NDM-1 with no inhibitor (●) and NDM-1 + TACN (□) are shown. Slope of the
483 initial rate represents the hydrolytic activity of NDM-1.

484 **Figure 6:** Time-dependent RMSD plots of A) $NDM1_{TACN,}$ B) $VIM\text{-}2_{TACN.}$ The complexes are represented

485 in black and the free enzymes in red.

486 **Figure 7:** Binding mechanism, illustrated by the interaction of docked ligand (TACN) at the active side

487 of NDM-1 (A) and VIM-2 (B).

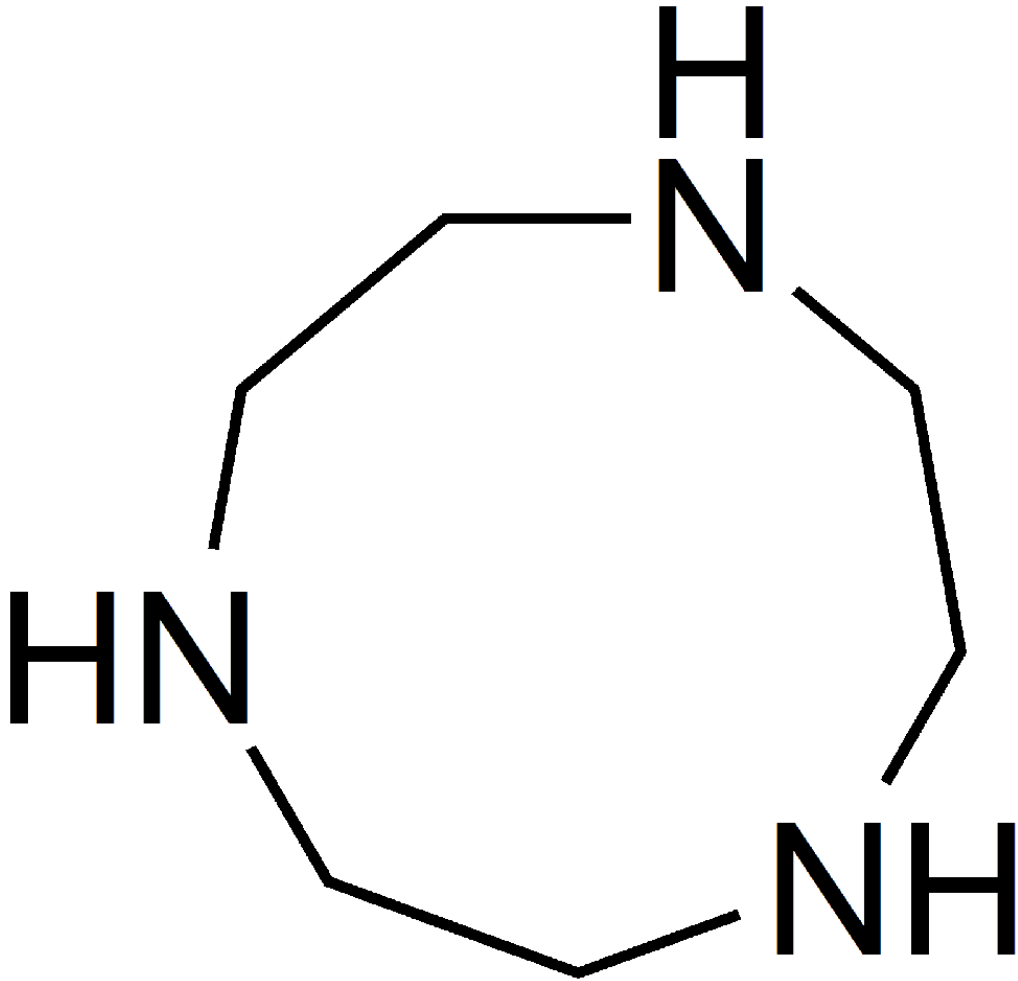
H
N
HN
NH

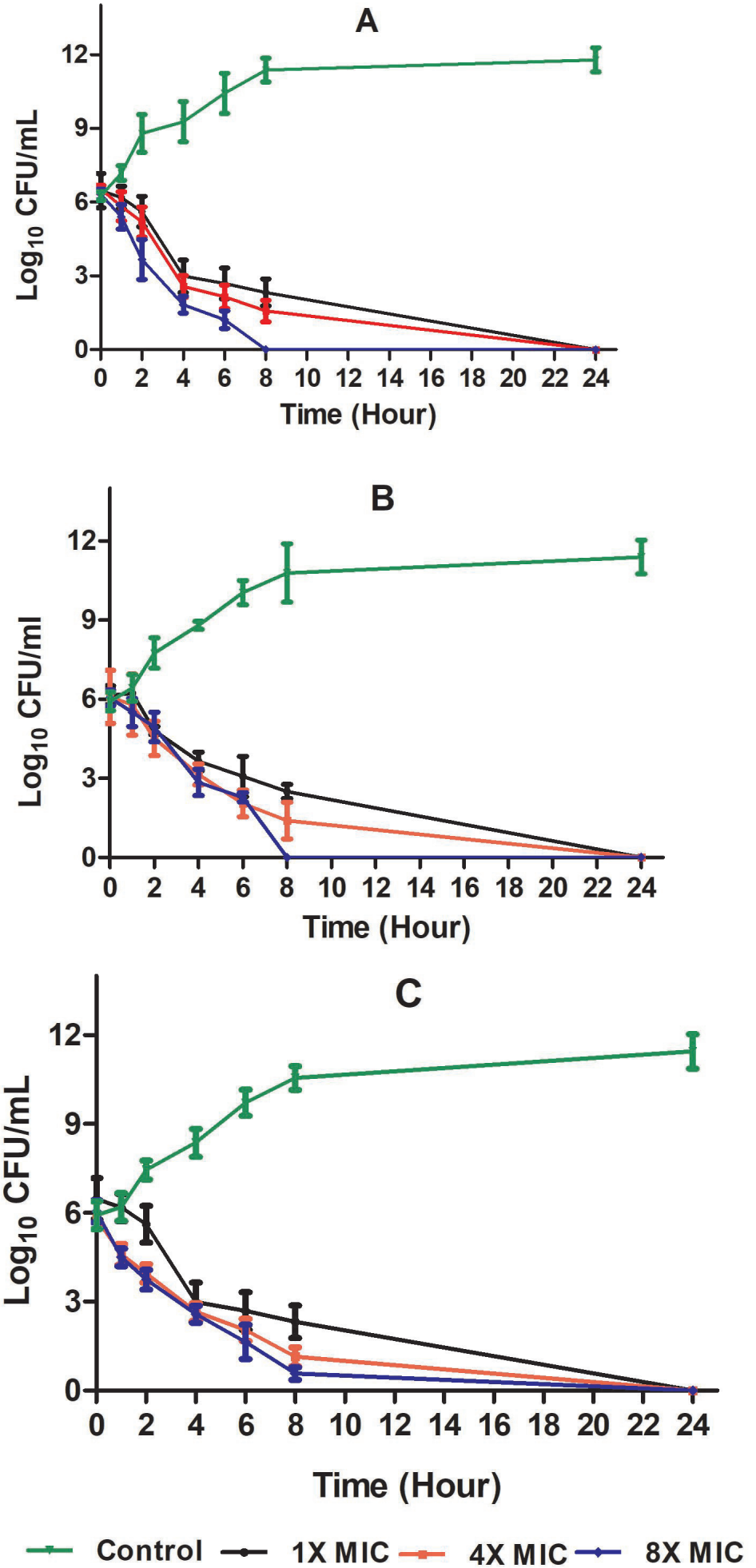
A
Log10 CFU/mL
12
9
6
3
0
0 2 4 6 8 10 12 14 16 18 20 22 24
Time (Hour)
B
Log10 CFU/ml
12
9
6
3
0
0 2 4 6 8 10 12 14 16 18 20 22 24
Time (Hour)
C
Log10 CFU/mL
12
9
6
3
0
0 2 4 6 8 10 12 14 16 18 20 22 24
Time (Hour)
Control
1X MIC
4X MIC
8X MIC

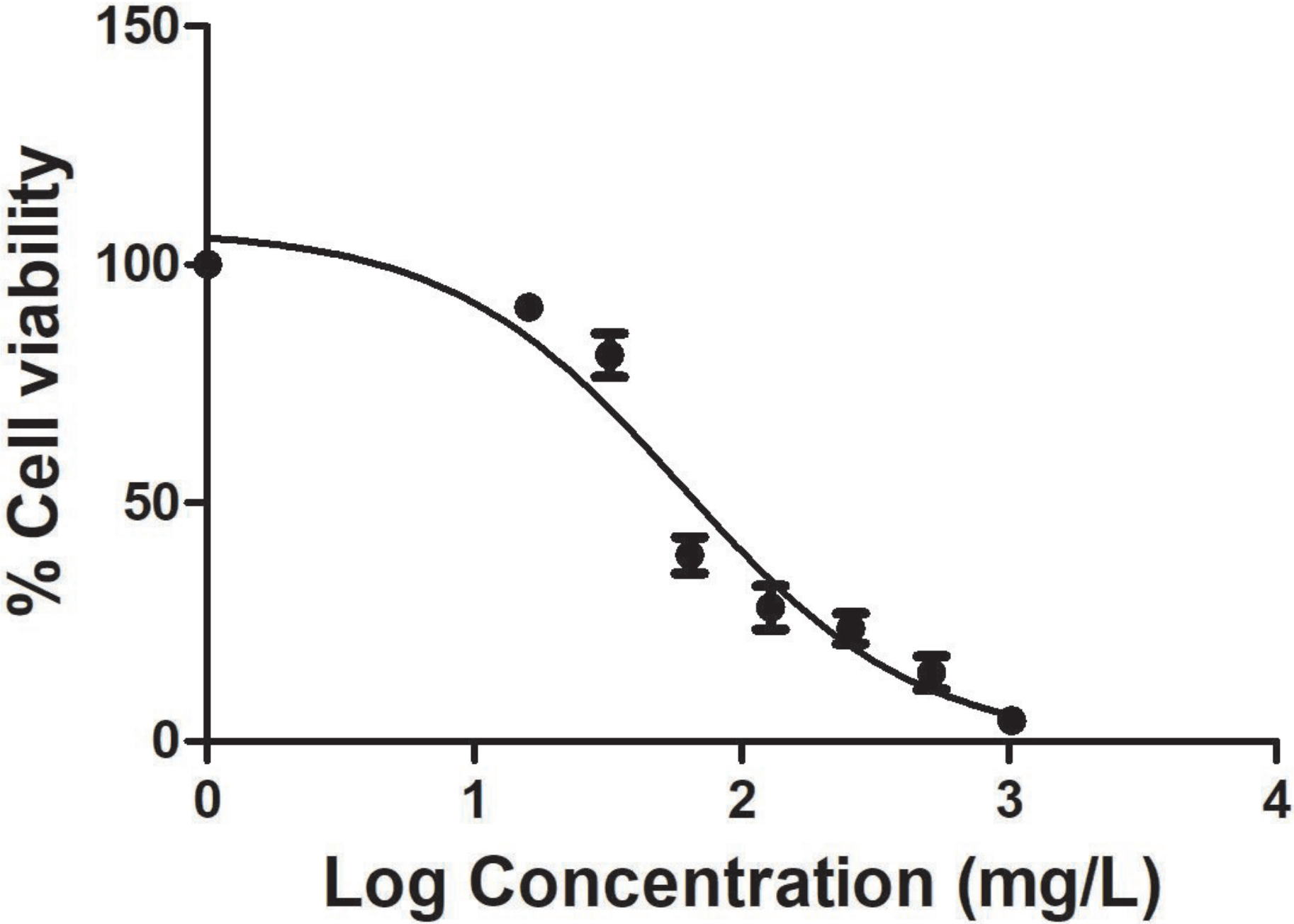
150
100
50
0
% Cell viability
0
1
2
3
4
Log Concentration (mg/L)

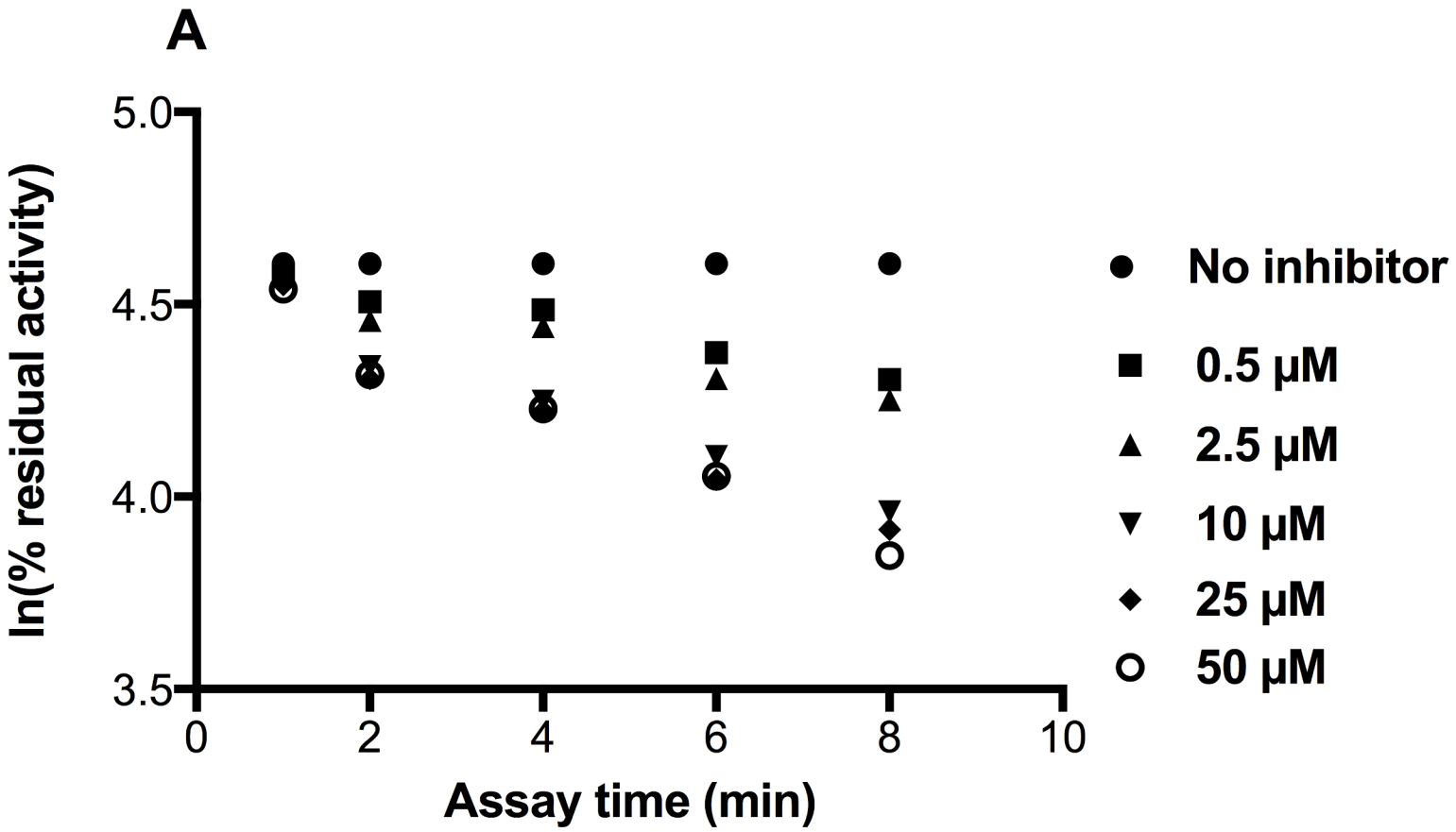
A
5.0
4.5
4.0
3.5
ln(% residual activity)
0
2
4
6
8
10
Assay time (min)
No inhibitor
0.5 μM
2.5 μM
10 μM
25 μM
50 μM

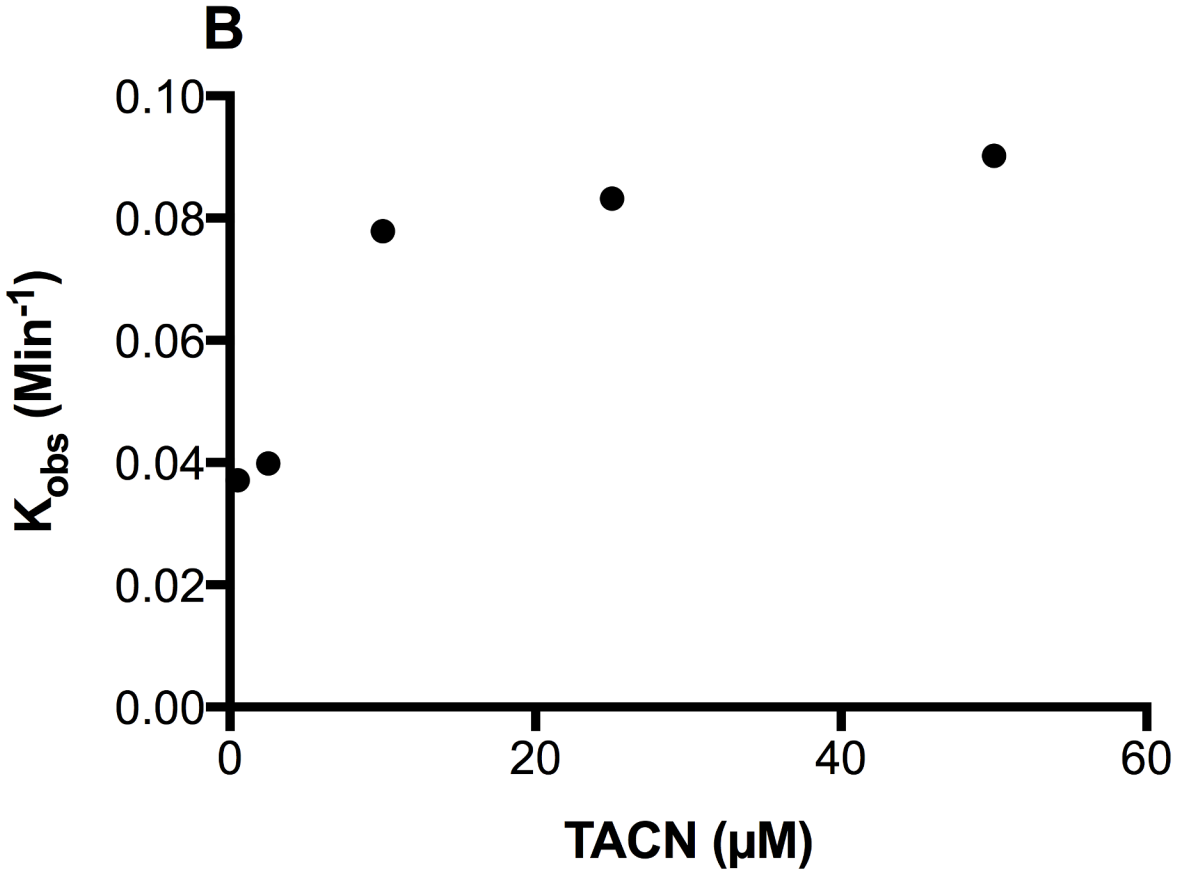
B
0.10
0.08
0.06
0.04
0.02
0.00
K_{obs} (Min^{-1})
0
20
40
60
TACN (μM)

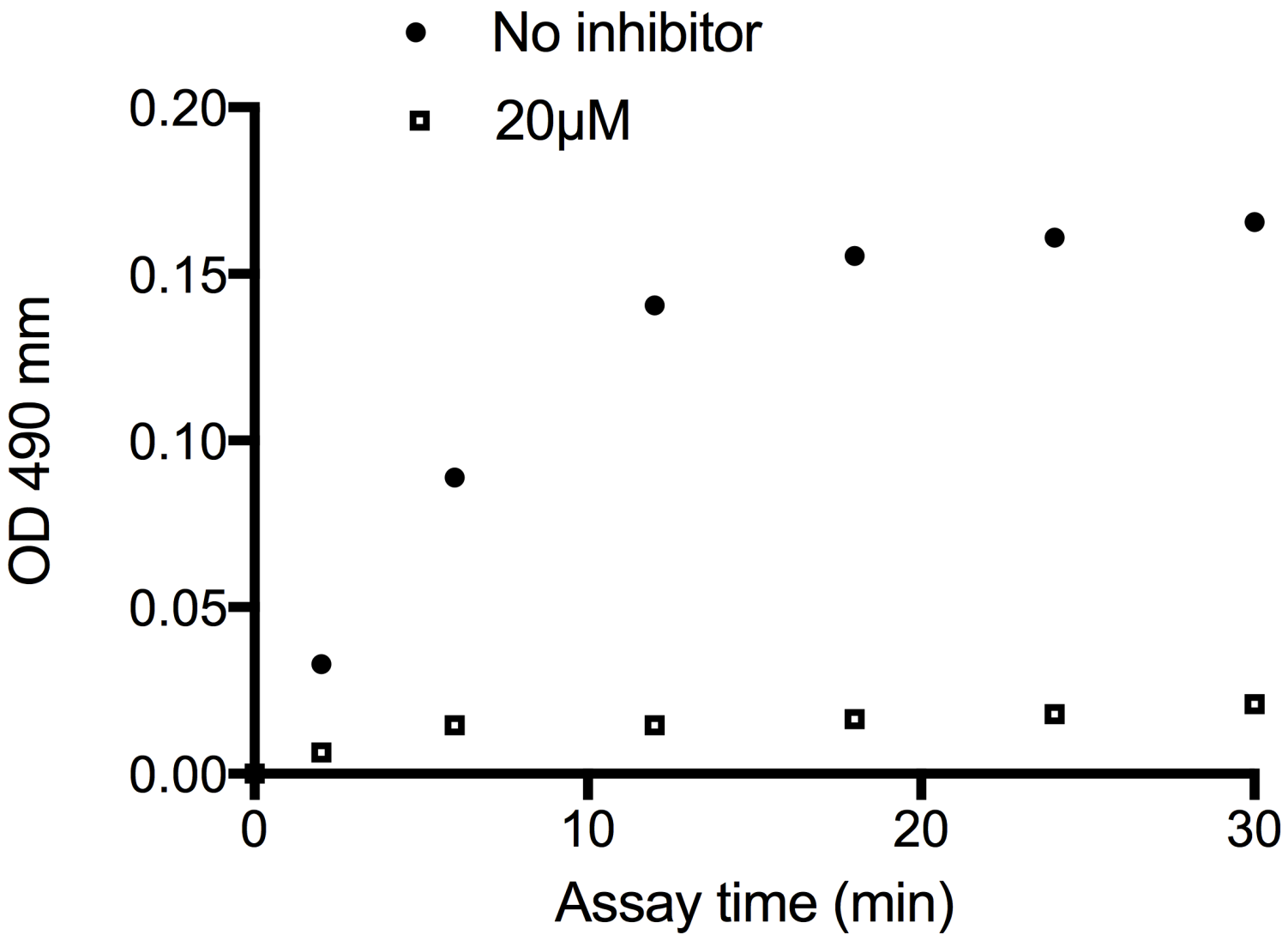
No inhibitor
20μM
0.20
0.15
0.10
0.05
0.00
OD 490 mm
0
10
20
30
Assay time (min)

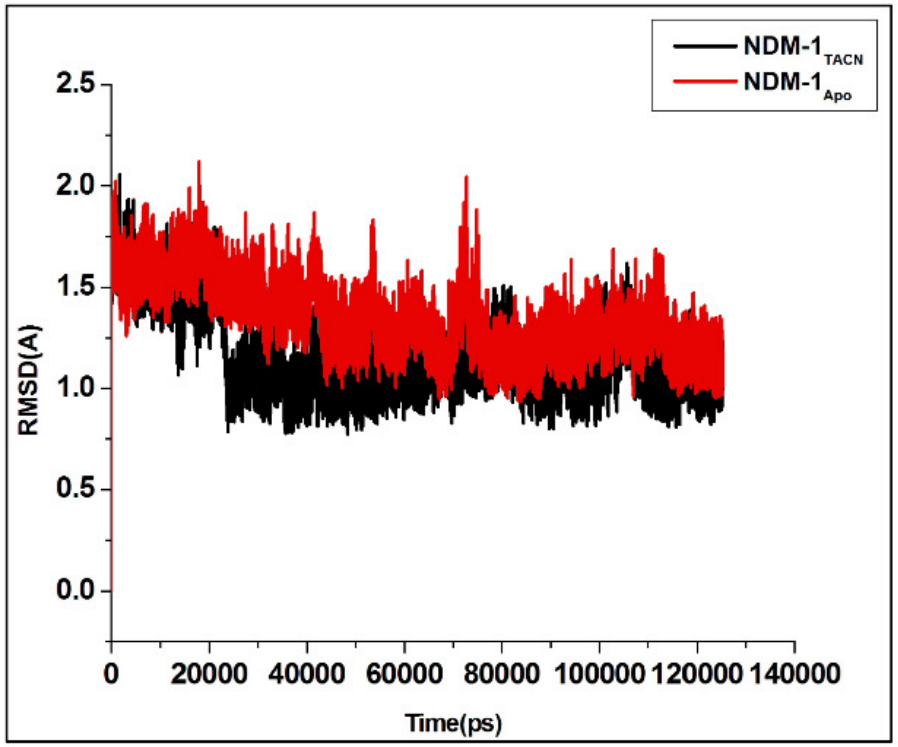
NDM-1TACN
NDM-1Apo
RMSD(A)
2.5
2.0
1.5
1.0
0.5
0.0
0
20000
40000
60000
80000
100000
120000
140000
Time(ps)

A

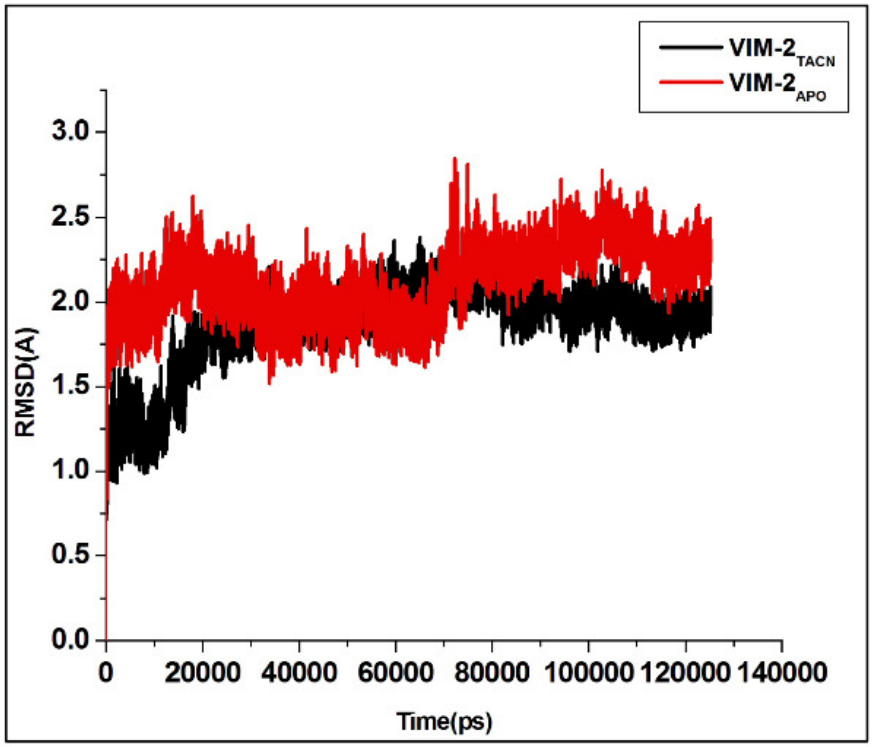
VIM-2TACN
VIM-2APO
RMSD(A)
3.0
2.5
2.0
1.5
1.0
0.5
0.0
0
20000
40000
60000
80000
100000
120000
140000
Time(ps)

B

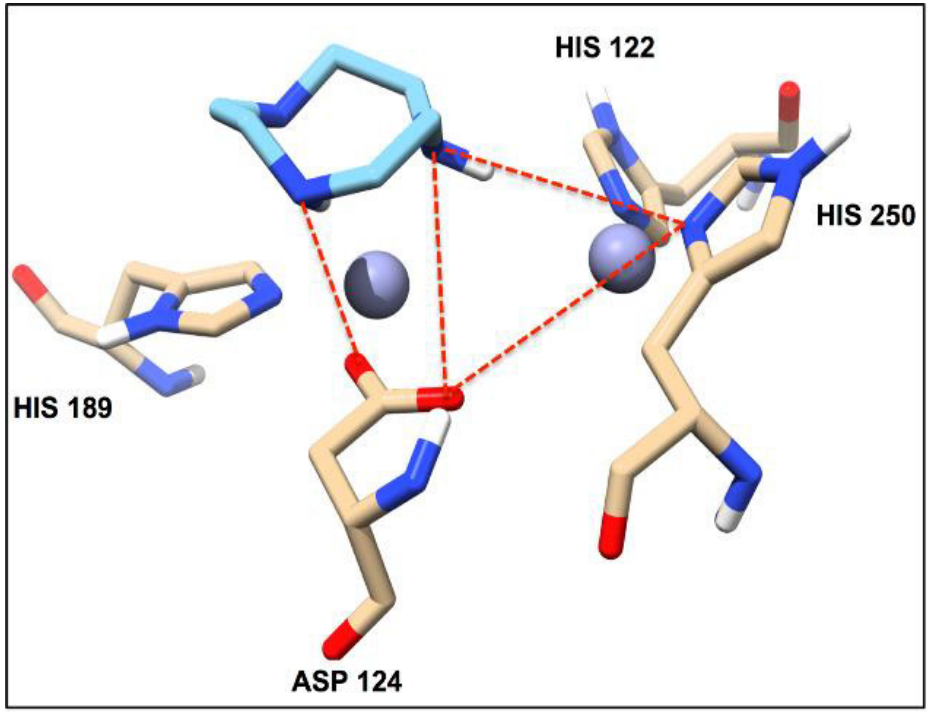
HIS 122
HIS 250
HIS 189
ASP 124

A

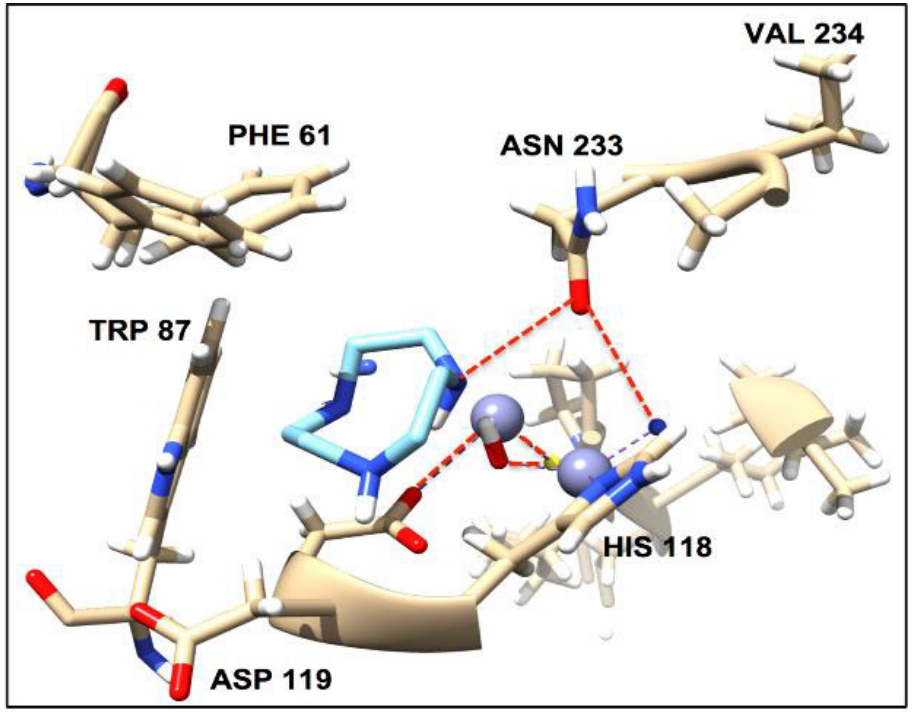
VAL 234
PHE 61
ASN 233
TRP 87
HIS 118
ASP 119

B